UNIVERSIDAD SAN FRANCISCO DE QUITO USFQ

Colegio de Ciencias e Ingenierías

On the Design of a Self-Powered Environmental Monitoring Station with AI

Diego Fernando Sandoval Calderón
Hugo Esteban Almeida Molina

Ingeniería Electrónica

Trabajo de fin de carrera presentado como requisito
para la obtención del título de
Ingeniero Electrónico

Quito, 19 de enero de 2024

UNIVERSIDAD SAN FRANCISCO DE QUITO USFQ

Colegio de Ciencias e Ingenierías

HOJA DE CALIFICACIÓN
DE TRABAJO DE FIN DE CARRERA

On the Design of a Self-Powered Environmental Monitoring Station with AI

Diego Fernando Sandoval Calderón

Hugo Esteban Almeida Molina

Nombre del profesor, Título académico **Alberto Sánchez, PhD**

Quito, 19 de enero de 2024

© DERECHOS DE AUTOR

Por medio del presente documento certifico que he leído todas las Políticas y Manuales de la Universidad San Francisco de Quito USFQ, incluyendo la Política de Propiedad Intelectual USFQ, y estoy de acuerdo con su contenido, por lo que los derechos de propiedad intelectual del presente trabajo quedan sujetos a lo dispuesto en esas Políticas.

Asimismo, autorizo a la USFQ para que realice la digitalización y publicación de este trabajo en el repositorio virtual, de conformidad a lo dispuesto en la Ley Orgánica de Educación Superior del Ecuador.

Nombres y apellidos: Diego Fernando Sandoval Calderón

Código: 00215294

Cédula de identidad: 1720592912

Lugar y fecha: Quito, 19 de enero de 2024

Nombres y apellidos: Hugo Esteban Almeida Molina

Código: 00211974

Cédula de identidad: 1722374251

Lugar y fecha: Quito, 19 de enero de 2024

TABLA DE CONTENIDO

TABLES INDEX

FIGURES INDEX

INTRODUCTION

In today's context, leveraging sensors for accurate data collection and employing artificial intelligence (AI) for processing information, has become indispensable in environmental research and working place conditions. The integration of technologies, such as raspberry pi-connected sensors, allows real-time monitoring to further process of air quality and pollutant levels. Applying AI techniques to these datasets not only enhances result accuracy but also can reveal hidden patterns and trends that might otherwise go unnoticed. This combination empowers researchers to gain a deeper understanding of how human activities impact the environment and public health, and contrariwise, how their variables affect human behavior. Accessing precisely processed data facilitates more effective environmental preservation and health promotion strategies, enabling informed decision-making in environmental management.

The United Nations Environmental Program (UNEP) underscores the severity of air pollution as a paramount global environmental threat, contributing to an estimated 7 million premature deaths annually. Examining the nexus between air pollution and climate change, the report, last updated in September 2023, provides a comprehensive overview of the current global state of air pollution, major pollution sources, health impacts, and national efforts to mitigate the crisis. Highlighting that 99% of the global population in 2019 lived in areas not meeting the strictest air quality guidelines [1].

Understanding the importance of addressing air pollution is essential as it directly impacts human health, the environment, and economies. Air pollution, high and low temperatures may produce health risks, leading to conditions like heart disease, respiratory issues, and more. Additionally, the economic costs associated with preventing and managing air pollution are substantial. Governments and industries are actively working on policy reforms and technological innovations to mitigate these challenges [2]. This is particularly important as Quito exceeds the air pollution limits allowed by the WHO and the Ecuadorian Air Quality Standard according to studies carried out by the Ministry of the Environment of Ecuador, the World Health Organization (WHO), the Pan American Health Organization (PAHO), some municipalities and universities [3].

The monitoring of temperature, humidity and CO_2 variables might give insight on the consequences of population, ecosystems and other. For example, monitoring variables such as humidity is crucial to understanding the climate and its impact on ecosystems. Regarding CO_2, its monitoring can serve as an indicator of climate change due to its contribution to global emissions [4]. Even monitoring environmental noise can be of great interest, since it can monitor different activities related to mobility and human behavior, thus acoustic contamination [2].

In general terms, the analysis and monitoring of all these variables has the objective of studying their possible impact on the environment or human health and development. [5]. Likewise, weather conditions can hinder work performance, leading to physical discomfort, irritability, and decreased productivity in high temperatures. Temperature may limit outdoor activities, affecting collaboration and teamwork. Overall, adverse weather can contribute to lower productivity and challenges in group dynamics.

The Universidad San Francisco de Quito (USFQ) is implementing an innovative project that deploys an advanced environmental monitoring station powered by artificial intelligence (AI). This station strategically places sensors to measure CO_2 levels, temperature, humidity and human traffic. Video processing with AI involves the application of artificial intelligence techniques to analyze and interpret visual content from videos. Using advanced algorithms, AI can identify patterns, objects, and even understand complex actions within video footage [6].

The importance of environmental and human behavior is clear, particularly to observe the variability of the different parameters in relation to humans. In addition, the study and collection of data in the Cumbaya Valley can be very useful to have a better understanding of the impact of climate change. In particular, the analysis of these environmental variables could serve to inform the USFQ community about the importance of caring for the environment and the impacts of climate change due to its activities and understand how workplace conditions affect human behavior.

SYSTEM ARCHITECTURE

Our proposal includes an electronic device built from the shelf components. Fig. (1) shows a high-level system architecture in which the main environmental sensors and power solution are presented.

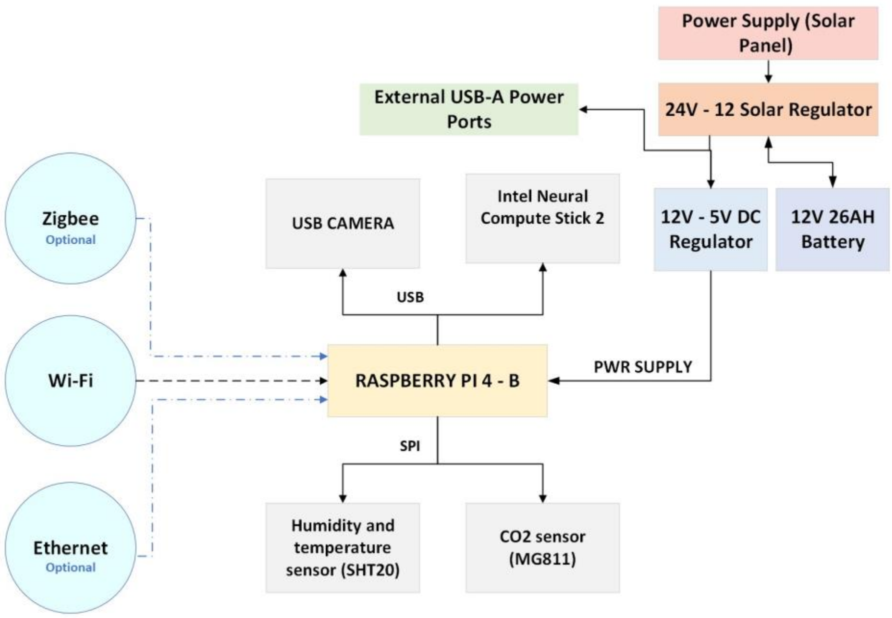

Figure 1. Monitoring Station Architecture

Power is supplied to the system by a 200W PV which is used to feed the electronics, charge a 12V-26Ah battery, and supply on-demand energy through external USB-A ports. There are internal USB-A and USB-C power ports that can be used to power external instruments that can be added in the future if new environmental variables are to be integrated, or for charging other devices. The use of an energy storage system (battery) allows the system to work continuously during low radiation conditions, such as for example during the night or due to bad weather, where the power generated doesn't supply the system. An additional 12V to 5V voltage regulator is used to feed the Raspberry and all the sensors connected to it. [7]

Regarding the process system, the architecture, Intel has previously developed products like the “Neural Compute Stick.” This is a USB device that contains a hardware accelerator for artificial intelligence (AI) and deep learning workloads. These sticks are designed to enable inference for AI models on devices that lack specialized hardware for such tasks. They provide an environment for running inferences at the edge or on peripheral devices, eliminating the need to rely on the computing power of remote servers or data centers. [6]

For communication, the system can work either connected to the internet through Wi-Fi, Ethernet or unattached when it is unable to hook-up due to it’s placement in remote locations or when the network present failures. In particular, Wi-Fi is a wireless communication standard that uses the IEEE 802.11n standard [8] and enables the creation of low-power energy efficient networks. It is well-suited for weather stations that aim to share data to the router.

There’s an optional connection which is not implemented but is considered for the future with Zigbee. Zigbee allows devices to form mesh networks to share data among each other and collaborate to transmit information along the communication chain. Additionally, its low power consumption and secure communication make it an excellent choice for further application.

A. Hardware

In this implementation only temperature, humidity and CO2 have been considered. The station includes the Neural Compute Stick 2 for the image recognition of persons and counts them through AI using an HD-USB camera. A complete description of each component is provided below, and Table I summarizes the main characteristic of each component.

Description	**Component**	**Power Supply** $[V]$	**Range**	**Interface**	**Consumption** $[mA]$	**Cost (USD$)**
Neural Stick 2	$NCS2$	5	7 modes[1]	5 V (Digital)	1500	$199
Temperature	SHT20	3.6	-40 to $125°C$	12 Bits (Digital)	15	$25
Humidity	SHT20	3.6	$50-95\%$	8 Bits (Digital)	15	$25
CO_2	$MG811$	3.3	$0-1000$ PPM	$1-3.3$ V (Digital)	1.6	$13
HD-USB Camera	$B086MM9FX4$	5	1080 MP	5 V (Digital)	300	$49

Table 1. Monitoring Station Component Characteristics and Approximate Cost

- **NCS2 Intel Neural Computer Stick 2:** This hardware accelerator designed to facilitate the development and deployment of deep neural networks (DNNs) at the edge for accelerating AI workloads connected though USB allows an easy integration with a variety of devices like the Raspberry Pi 4 to improve performance and efficiency of the CPU for image recognition with AI tasks. The module helps with the identification of people in the environment. The module consumes 2500mA, making it suitable for battery-powered or resource-constrained devices connected directly to the USB port of the board. The module is presented in Fig. (2.a). [9].
- **SHT20Temperature and Humidity Sensor Module:** This sensor module measures temperature in the environment with an accuracy of ±2 °C and humidity with an accuracy of 5% which perfectly suits this application. The module can produce readings in °C or °F as a digital voltage ranging from 3.6V . The device can sink up to 15mA. In this system, the voltage supply is 3.6V. Fig. (2.b) shows the module. [10].

- **MG811 CO2 Sensor Module:** This is a sensor module which is highly sensitive to CO2 and less sensitive to alcohol and CO, with a low humidity and temperature dependency. It is working voltage ranges from 1.0V to 3.3V and has a 0.16mA current consumption. The module is supplied with 3.3V directly from the Arduino board. Fig. (2.c) shows the module. [11].
- **B086MM9FX4 HD-USB Camera Web:** The Web camera is required to give the image which the AI is going to be performed collected the frame giving the information to the NCS2 to do image recognition in the environment. This module can work with a supply voltage of 5V and has a 300mA current consumption in the worst scenario where the camera needs to adapt the light. Fig (2.d)
- **Raspberry Pi 4:** To keep the system low cost, and user-friendly specially working with the NCS2 for the AI image recognition which is effective and low-cost into the small single-board computers (SBCs) which is based on ARM Cortex-A72 processor. This board allows for sufficient computational capabilities and has a rich number of IO's and analog channels for this project including ports with high functionality for communication like Bluetooth, Ethernet and Wi-Fi.

Figure 2. Monitoring Station Components

The power supply solution draws energy from a 200W PV and can charge the energy storage system (12V 26Ah battery) and provide sufficient energy to supply the Raspberry Pi 4 board and all the module components presented in annex B. The solution also feeds a USB port module, which can be used to power external devices. The battery has been sized to last about 24 hrs supplying all the considered modules. Table II presents the system current consumption.

Instrument	**Consumption** $[mA]$
Rasbperry Pi 4	1000
All modules	1816.6
Total Power Consumption per hour	2816.6$[mA]$
Approximate System Backup-Time	24 hr.

Table 2. Monitoring Station Current Consumption

A system depiction is presented in Fig. (3). This figure mimetices the hardware connections and interfaces.

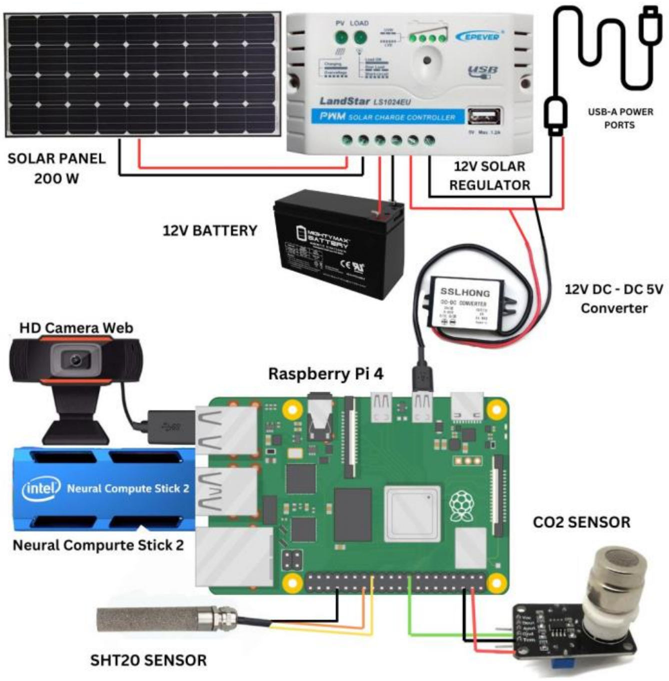

Figure 3. System Internal Connections

For the system enclosure we use a metallic box with adapted for an IP65 certification in which it is possible to protect the Battery, the rectifier and the Raspberry Pi 4 board from the climatic conditions where sensor modules are placed within the board box and are securely wired using appropriate connectors. The modules are sufficiently protected from environmental conditions such that they will not get in direct contact with water. It is expected however that these modules will eventually fail, but the system is designed so it is easy to replace them though an easy plug and play for the main components.

B. Software

The use of the Raspberry Pi 4 platform greatly facilitates the programming of the system using Ubuntu. The system comprises four main software tasks: data-acquisition, data, data-storage, and communication.

1. **Data-Acquisition and Processing:** The sensor modules employ either an analog or digital interface. Data acquisition occurs at a rate of 1 sample per second, processed as a 5- minute average, and accurately timestamped using the board's Real-Time Clock. It's crucial to emphasize that, in this context, population count compilation refers to the total number of individuals present in the environment throughout the entire day.

   Python is used to manage the sensor modules, streamlining integration through libraries and packages that enable communication via SPI com-ports of the Raspberry Pi 4. The software for the sensor modules conducts signal transformation to derive precise values from the sensors.

   To implement AI, the Intel®OpenVINO Toolkit serves as an open-source solution tailored for optimizing and deploying AI inference across diverse domains. It caters to applications ranging from computer vision, automatic speech recognition, and natural language processing to recommendation systems and generative AI.

The recently released version, OpenVINO 2023.2, introduces several features, improvements, and deprecations aimed at enhancing the developer experience.

Upon AI identification, we implement Python code employing libraries provided by OpenVINO. The base model, implemented with a focus on high-resolution images, integrates a USB-camera. The USB camera requires the use of CV2 drivers on Ubuntu to recognize the camera on specific ports. [12].

The system operates by uploading frames captured by the camera, which are then processed for recognition. The model employs mesh-based identification, delineating a zone of interest in pixels where the AI concentrates its focus. Initially, it ensures and focuses on the broader environmental view to gauge object distance for an optimal zone of interest and improved AI performance. Subsequently, the focus narrows down to the delimited zone, enhancing performance on a new pixel area rather than the entire video range. This refined range captures static elements of the environment, facilitating the identification of any abnormal objects in the analyzed frame. The NCS2 model takes full advantage of the Video Processor Unit (VPU), thereby optimizing CPU usage for other tasks on the Raspberry Pi 4. When a person is recognized, using the tracking model the system identifies the detected person and simultaneously counts it alongside in the frame.

The implemented system uses ResNet-50, which is a convolutional neural network (CNN) architecture designed for image classification tasks. Its key feature is the use of residual blocks, incorporating shortcut connections to mitigate the vanishing gradient problem in deep networks.

The neural network is designed for video action recognition, that captures information at different temporal speeds in a deep residual neural network with 50 convolutional layers. For ResNet-50 this combination excels in recognizing actions in video sequences. This network is typically implemented using the training model in PyTorch and is integrated for its ability to handle intricate video details converted by OpenVINO for efficient inference. [13].

2. **Data-Storage:** The Raspberry Pi 4 employs a memory card (Micro SD) to store its program and interface with storage. The software for this application takes up about 31.2 gigabytes. The card can store considerable information for extended periods presented in table II, which is especially useful when the communication link is not available.

Micro SD Size $[GB]$	**Available Storage** $[Days]$
64	1939.39
128	7,757.56
256	15,215.12
512	31,030.14

Table 3. Micro SD size for storage

It is possible to keep track of every person count during the day, but exporting this amount of data exceeds the storage capacity of the card. This not only makes it challenging to store all that information but can also slows down the Raspberry Pi 4. The AI functions require a considerable amount of resources and generate a continuous exchange of data with the memory card, which affects the overall performance.

Due to this reason, an external database server has been setup to store data coming from the monitoring station. The server is internet compatible, which means it can be accessed by Wi-Fi or ethernet. Future work can implement remote storage using a cloud service.

3. **Communications:** The main code contains extensions to facilitate the connection with MySQL from Ubuntu and Python. The server and the monitoring station must be in the same network for the system to connect.

   Since the Raspberry Pi 4 does not have an internal battery, the timestamp can be lost id the device suffers a power failure. The system time is automatically updated as long as the system is able to connect to internet clocks through the operating system.

   The Raspberry program is able to send three commands to the database through the link: *update, insert* and *get*. The *update* function modifies the measured variables. This ensures that the system knows which data to export based on the current daytime, which becomes crucial in case of any server blackout or unforeseen circumstances. The program continues running seamlessly, adapting to disruptions and maintaining functionality or connectivity. Afterwards, *Insert* exports data in the format: (count, date, last-update) according to the table created in MySQL. Finally, the *get* command archives the count of persons. Only the total number of people count by day or each time the count increments is exported to the database. Currently the system sends the total day count. This can be configured by the user according to the amount of data required.

EXPERIMENTATION AND RESULTS

The current weather information in Quito, Ecuador, was sought on the AccuWeather page. Detailed comparisons were conducted between the data obtained from this source and the readings from our environmental sensor. During the analysis, a notable alignment was observed between the sensor results and the weather forecasts provided by AccuWeather. This comparison is crucial in evaluating the accuracy and reliability of our sensor measurements [14].

A. Connection Box

The Connection Box is a sealed enclosure designed to prevent water ingress. Equipped with IP65-rated protectors, it ensures watertightness for cables entering or exiting the box. Internally, it is securely fastened with screws to enhance its sealing. Aesthetically, it presents a neat and well-maintained appearance, providing a robust and visually pleasing solution to safeguard electrical connections in outdoor or damp environments show in Fig. 4 and 5

Figure 4. Connections Box

Figure 5. Box on the outside

B. Temperature Results

The temperature graph reveals two distinct datasets: one sourced from a sensor and the other from an online platform. The noteworthy observation is the striking similarity in the range of values between the two sets of data. It is important to acknowledge that the web-based information provides precise values, whereas the sensor data demonstrates a higher degree of accuracy, as shown in Fig. 6

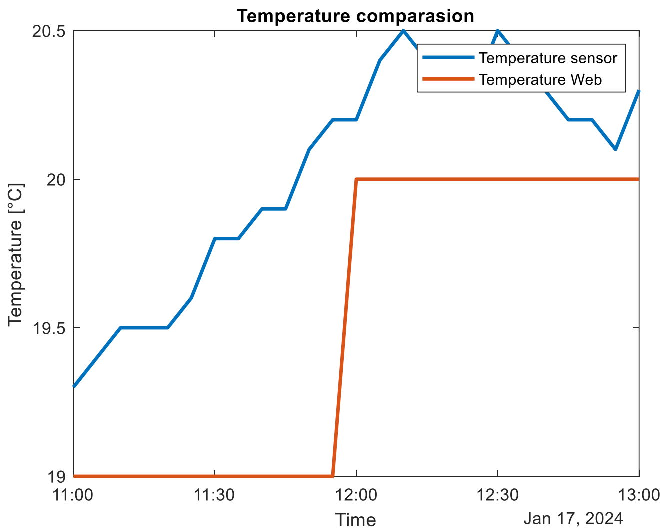

Figure 6. Temperature results from sensors vs web

C. Humidity Results

The humidity graph also presents two sets of data: one obtained from a humidity sensor and the other from an online source. Notably, a discernible pattern emerges, indicating an inverse relationship between humidity and temperature. As the temperature increases, the humidity levels tend to decrease. Fig 7

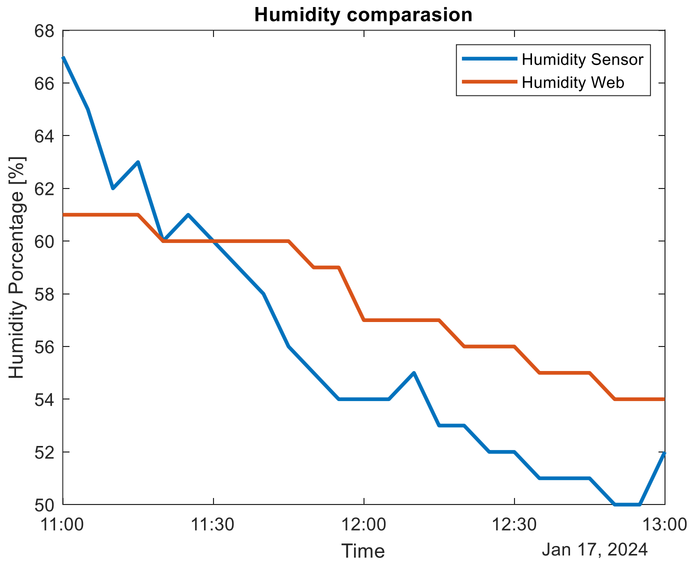

Figure 7. Humidity results from sensors vs web

D. CO2 Results

The concentration of carbon dioxide (CO_2) tends to increase in the presence of people in a confined space due to human respiration. When people exhale, they release carbon dioxide as part of the respiratory process. In spaces with inadequate ventilation, CO_2 can accumulate over time, especially in closed environments or those with poor ventilation systems [15].

Elevated CO_2 levels in the air can not only affect air quality, but also have implications for the health and well-being of individuals. Prolonged exposure to high CO_2 levels can lead to symptoms such as headaches, fatigue, lack of concentration, and overall discomfort, contributing to what is known as the sick building syndrome. Fig. 8

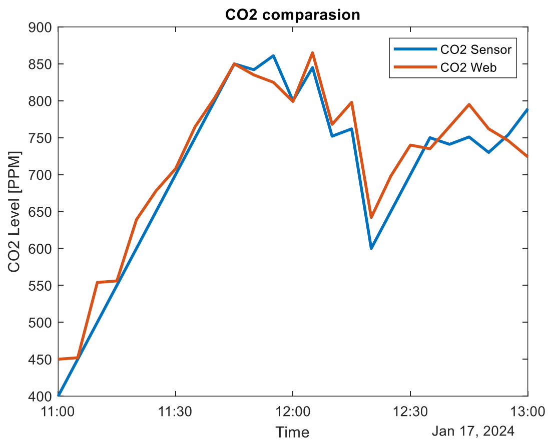

Figure 8. CO2 results from sensors vs web

E. Video Processing Results

The system can display in real-time the results of the video processing coming from the NN, emphasizing the frame mask and region of interest (roi) as presented in Fig. 9. Notably, the implemented model demonstrates robust performance even under challenging conditions, such as very opaque visibility, which exemplifies an extreme case.

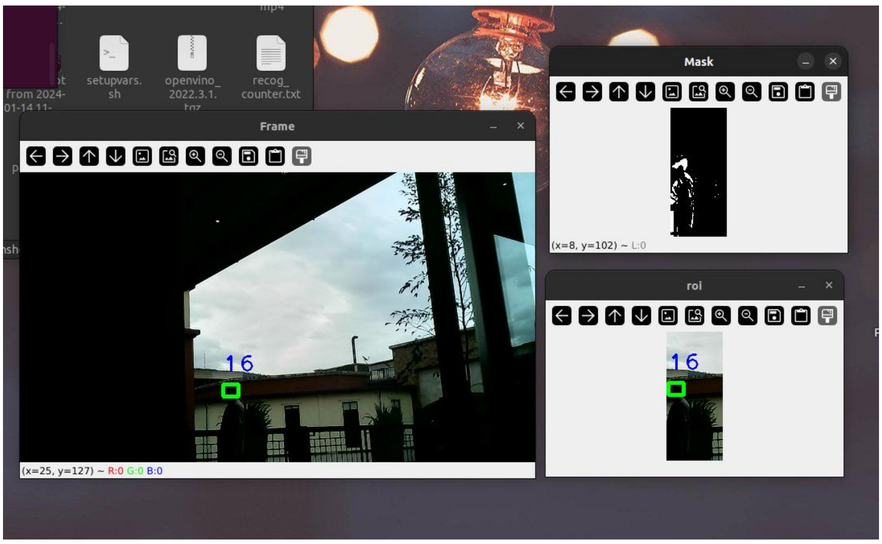

Figure 9. AI person Recognition and counting

It's important to highlight that the information is not only processed for accurate person counting but also for persistent display on the screen. This ensures that the results are not only dynamically generated but also recorded for ongoing reference.

Moreover, the system's ability to operate effectively under extreme visibility conditions showcases its resilience and reliability. As we continue to refine and enhance the AI model, we're exploring additional features that could contribute to the overall functionality of the system.

F. MySQL Server Tables

With the implemented system for the Raspberry Pi 4 the results can be visualized in real-time on MySQL Server where sensor data can be displayed, and the count of persons as illustrated in Fig. 10

id	temperature	co2	humidity	datetime
1	19,3	400	67	2024-01-17 11:00:00
2	19,4	450	65	2024-01-17 11:05:00
3	19,5	500	62	2024-01-17 11:10:00
4	19,5	550	63	2024-01-17 11:15:00
5	19,5	600	60	2024-01-17 11:20:00
6	19,6	650	55	2024-01-17 11:25:00
7	19,8	700	60	2024-01-17 11:30:00
8	19,8	750	59	2024-01-17 11:35:00
9	19,9	800	58	2024-01-17 11:40:00
10	19,9	850	51	2024-01-17 11:45:00
11	20,1	842	50	2024-01-17 11:50:00
12	20,2	861	51	2024-01-17 11:55:00
13	20,2	800	52	2024-01-17 12:00:00

Figure 10. MySQL Sensors Table

On the other table, the results of the people count can be visualized in real-time on MySQL Server showing the total count of persons by the day as illustrated in Fig. 11

id	count	date	last_updated
1	156	2024-01-15	2024-01-15 23:44:40
2	10	2024-01-16	2024-01-16 00:34:34
19	17	2024-01-17	2024-01-17 10:13:53

Figure 11. MySQL People Count Table

CONCLUSIONS AND FUTURE WORK

This system serves as a low-cost environmental monitoring solution designed for different locations, whether accessible or remote. It can store measurements locally or transfer them via IoT's communication interface. It's especially useful in areas lacking readily available energy. The system incorporates a power supply solution with photovoltaic (PV) panels and an energy storage system. The deployment of this station is targeted for both urban and environmentally sensitive locations holding an IP65 certification. Also verified for heavy rainfall and dusty environments, where the principal use of low-cost common sensors is easy to replace in case of external damage and has easy replacement. Measurements obtained were compared with web pages, proving that the data range is correct.

The robust box design ensures prolonged operation, due to the energy storage solution with low power consumption of The Raspberry Pi 4 using AI based system. Allowing real-time visualization of the results of the sensors and the people count through a MySQL Server tables, preventing loss of the data from a black-out and for an easy extraction of the data for further analysis.

For future work include other sensors for more environmental information, also develop a user-friendly graphical interface to read data on a web page (like Arduino Cloud or Web design). Additionally, employ artificial intelligence for data processing into the server to predict weather conditions. This continuous improvement will enhance the system's functionality and contribute to its effectiveness in environmental monitoring.

REFERENCES

[1]. World Health Organization. (2014). "7 million deaths linked to air pollution," Department of Public Health, Environmental and Social Determinants of Health (PHE), 63. https://doi.org/10.19053/20278306.v8.n2.2018.7971

[2]. Kumar, S., & Katoria, D. (2013). Air Pollution and its Control Measures. International Journal of Environmental Engineering and Management, 5(5), 445-450.

[3]. Loaiza, Y. (2023). El aire contaminado que respiramos en el Ecuador. https://gk.city/2019/09/16/aire-contaminado-ecuador-ciudades/

[4]. AccuWeather. (2024). Tiempo Actual Quito. https://www.accuweather.com/es/ec/quito/129846/current-weather/129846

[5]. Pal, S., Bandyopadhyay, M., Chowdhury Kolay, S., & Chattopadhyay, S. (2023). Remote Air Quality Sensing and Temperature Monitoring System using GSM for Smart City Application. In 2023 International Conference on Artificial Intelligence and Smart Communication (AISC) (pp. 338-342). https://doi.org/10.1109/AISC56616.2023.10085138

[6]. Ceccato, P., Fernandes, K., Ruiz, D., & Allis, E. (2014). Climate and environmental monitoring for decision-making. Earth Perspectives, 1(16), 1-22. https://doi.org/10.1186/2194-6434-1-16

[7]. Generalitat Valenciana. (2008). Ozono Troposférico y Calidad del Aire. (Enrique Mantilla, Nuria Castell, Rosa Salvador, César Azorín, Millan Millan, José Miró, & Lucía Juan).

[8].Horev, R. (2018). SlowFast Explained: Dual-mode CNN for Video Understanding. https://towardsdatascience.com/slowfast-explained-dual-mode-cnn-for-video-understanding-8bf639960256

[9]. Kucukhuseyin, O. (2021). Monitoring and indoor air quality. https://www.rehva.eu/rehva-journal/chapter/co2-monitoring-and-indoor-air-quality

[10]. IEEE. (2020). IEEE Standard for Low-Rate Wireless Networks. IEEE Std 802.15.4-2020 (Revision of IEEE Std 802.15.4-2015). https://doi.org/10.1109/IEEESTD.2020.9144691

[11]. Aleksandrova, O., & Bashkov, Y. (2020). Face recognition systems based on Neural Compute Stick 2, CPU, GPU comparison. In 2020 IEEE 2nd International Conference on Advanced Trends in Information Theory (ATIT) (pp. 104-107). https://doi.org/10.1109/ATIT50783.2020.9349313

[12]. SENSIRION. (2022). SHT20 Temperature and Humidity sensor IC. Ver.5.

[13]. Rajguru Electronics (I) Pvt. Ltd. MG-811 Carbon Dioxide Sensor Module.

[14]. Intel Corporation. (2023). OpenVINO API 2.0 Transition Guide — OpenVINO documentation. https://docs.openvino.ai/2023.2/openvino_2_0_transition_guide.html

[15]. Luo, F. L. (2011). Design of solar-panel energy system. In 2011 6th IEEE Conference on Industrial Electronics and Applications (pp. 2304-2309). https://doi.org/10.1109/ICIEA.2011.5975976

ANNEX A: USER GUIDE

To set up the Raspberry Pi 4 when it is turn-on from the Terminal as shown in Fig. (A-1), its important to enter the environment generated within the system with the command *source openvino_env/bin/activate*. Then within it go to the folder *cd Downloads* selecting the name of the project *cd object_tracking* and run the program with the python command *python processvideodb.py*, with which the program runs. You will be able to see from the terminal how measured data is printed in real time.

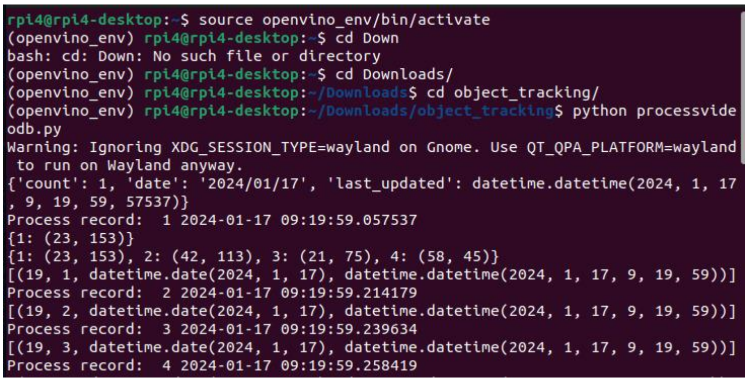

Figure A-1. System Program set-up

The connection of the station with the MySQL server is accomplished as long as both entities are in the same network as is presented in Fig. (A-2).

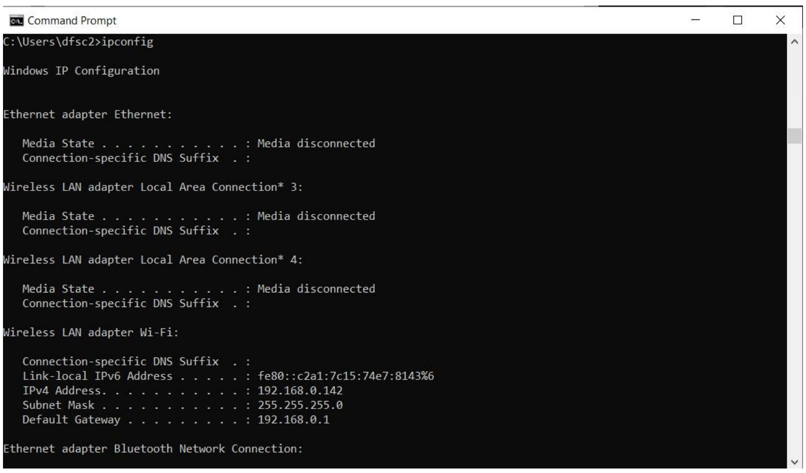

Figure A-2. Server IP Verification

It is important to verify the address typed into the program to recognize the destination of the data. While the program is running, we can see on the CMD of the server the verification of connection between the Raspberry Pi 4 as presented in Fig. (A-3).

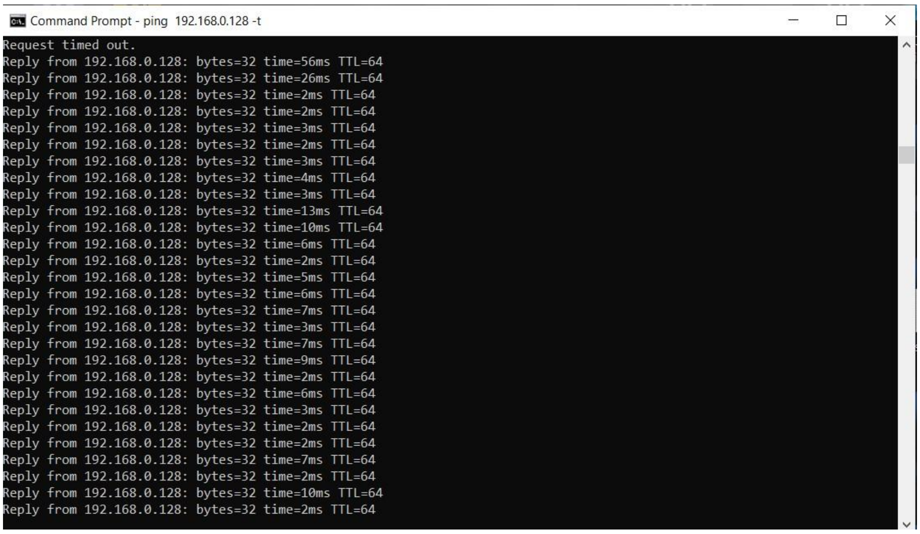

Figure A-3. IP link Server-Raspberry Pi 4

At this point, the connection if there are no connection errors, which means that data is being received without problem as presented in Fig. (A-4).

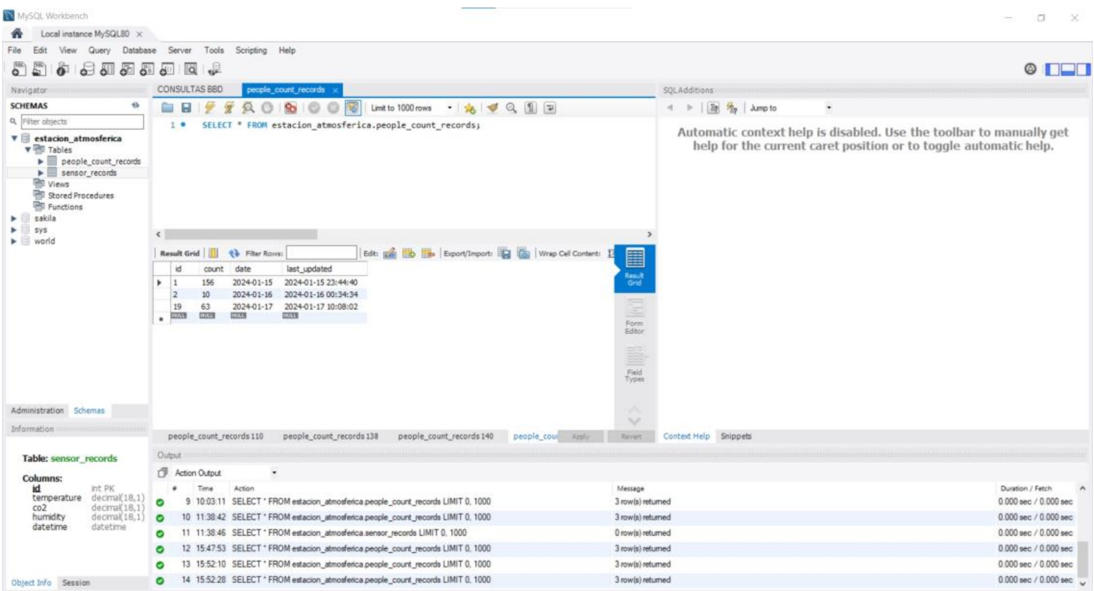

Figure A-4. MySQL Server Interface recognition

ANNEX B: UNIFILAR DIAGRAM

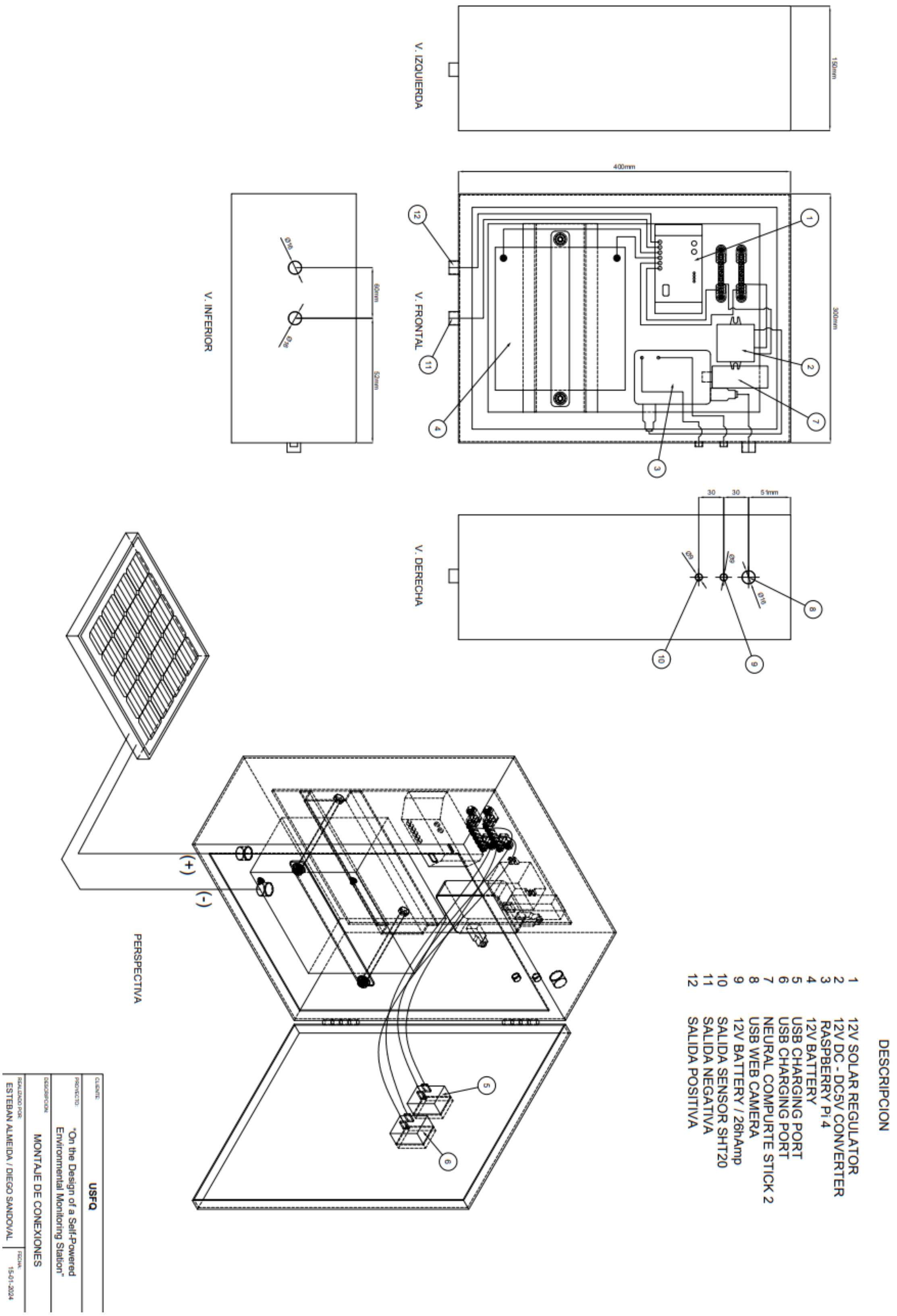

ANNEX C: CO2 SENSOR DATASHEET

MG811 CO2 Sensor

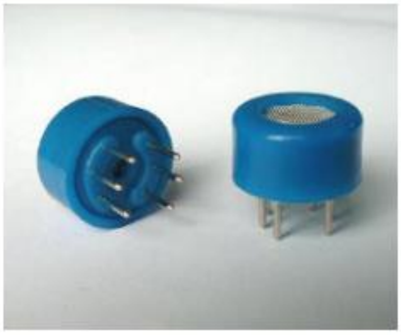

Features

Good sensitivity and selectivity to CO_2
Low humidity and temperature dependency
Long stability and reproducibility

Application

Air Quality Control
Ferment Process Control
Room Temperature CO_2 concentration Detection

Structure and Testing Circuit

Sensor Structure and Testing Circuit as Figure, It composed by solid electrolyte layer（1）,Gold electrodes（2）,Platinum Lead（3）, Heater（4）, Porcelain Tube（5）, 100m double-layer steeless net（6）, Nickel and copper plated ring（7）, Bakelite (8) , Nickel and copper plated pin（9）。

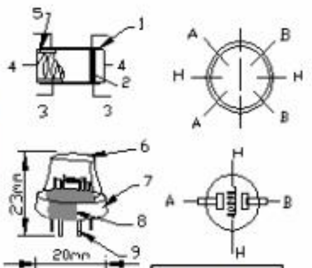

Figure 1A

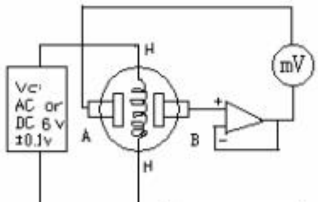

Figure 1B

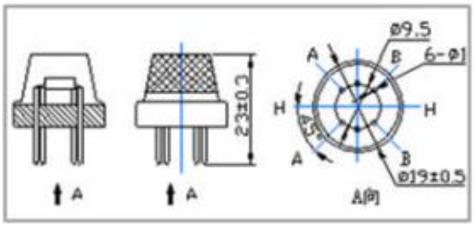

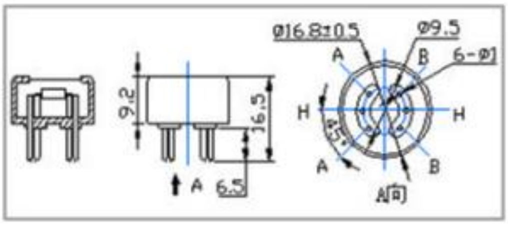

Working Principle

Sensor adopt solid electrolyte cell Principle , It is composed by the following solid cells：

Air , Au|NASICON|| carbonate|Au, air , CO_2

When the sensor exposed to CO_2 , the following electrodes reaction occurs：

Cathodic reaction：$2Li^+ + CO_2 + 1/2O_2 + 2e^- = Li_2CO_3$

Anodic reaction：$2Na^+ + 1/2O_2 + 2e^- = Na_2O$

Overall chemical reaction：$Li_2CO_3 + 2Na^+ = Na_2O + 2Li^+ + CO_2$

The Electromotive force（EMF）result from the above electrode reaction, accord with according to Nernst's equation: :

$$EMF = Ec - (R \times T) / (2F) \ln (P(CO_2))$$

$P(CO_2)$—CO_2--- partial Pressure   Ec—Constant Volume   R—Gas Constant volume

T— Absolute Temperature （K）F—Faraday constant

From Figure 1B , Sensor Heating voltage supplied from other circuit , When its surface temperature is high enough , the sensor equals to a cell, its two sides would output voltage signal ,and its result accord with Nernst 's equation。 In sensor testing, the impedance of amplifier should be within 100—1000GΩ , Its testing current should be control below 1pA.

Specifications :

Symbol	Parameter Name	Technical	Remarks
V_H	Heating Voltage	6.0±0.1 V	AC or DC
R_H	Heating Resistor	30.0±5%Ω	Room Temperature
I_H	Heating Current	@200mA	
P_H	Heating Power	@1200mW	
Tao	Operating Temperature	-20—50	
Tas	Storage Temperature	-20—70	
? E?M F	Output	30—50mV	350—10000ppmCO2

Sensitivity :

Figure 2 Shows gas sensor sensitivity curve. :

Conditions:

Tem : 28℃、

RH : 65%、

Oxygen : 21%

EMF: sensor EMF under different gas and concentration .

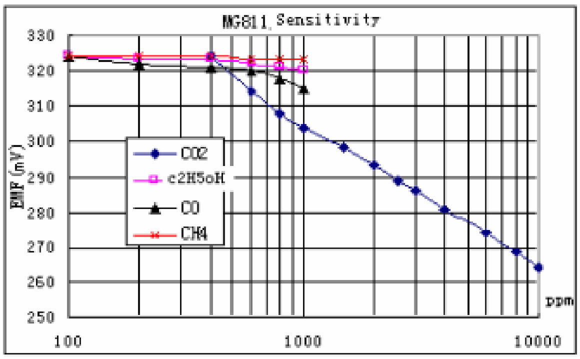

Response and Resume Characteristic :

Figure 3 shows Solid electrolyte sensor response and resume characteristics.

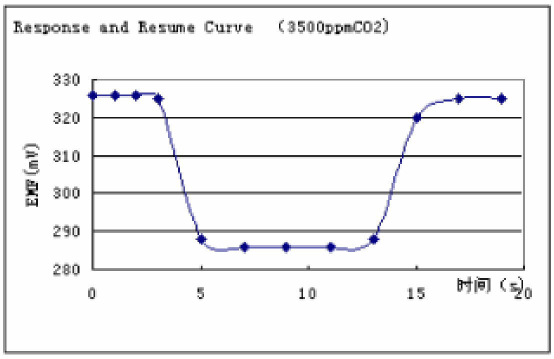

Temperature and Humidity Dependency :

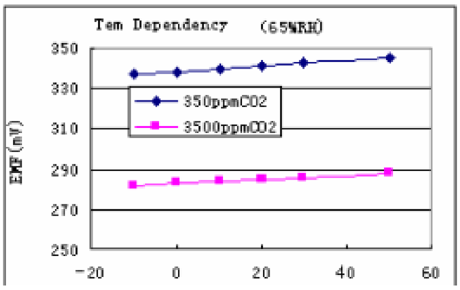

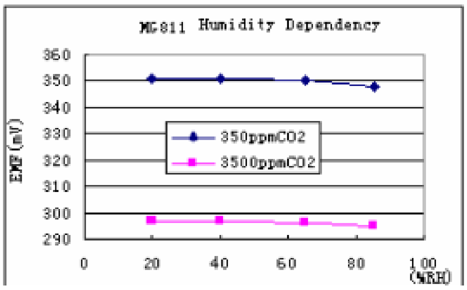

ANNEX D: SHT20 DATASHEET

SENSIRION
THE SENSOR COMPANY

Datasheet SHT20

Humidity and Temperature Sensor IC

- Fully calibrated
- Digital output, I²C interface
- Low power consumption
- Excellent long-term stability
- DFN type package – reflow solderable

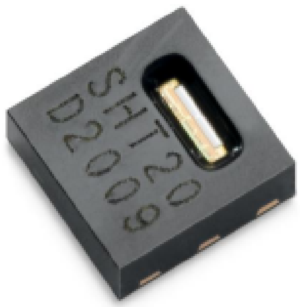

Product Summary

The SHT20 humidity and temperature sensor of Sensirion has become an industry standard in terms of form factor and intelligence: Embedded in a reflow solderable Dual Flat No leads (DFN) package of 3 x 3mm footprint and 1.1mm height it provides calibrated, linearized sensor signals in digital, I²C format.

The SHT2x sensors contain a capacitive type humidity sensor, a band gap temperature sensor and specialized analog and digital integrated circuit – all on a single CMOSens® chip. This yields in an unmatched sensor performance in terms of accuracy and stability as well as minimal power consumption.

Every sensor is individually calibrated and tested. Lot identification is printed on the sensor and an electronic identification code is stored on the chip – which can be read out by command. Furthermore, the resolution of SHT2can be changed by command (8/12bit up to 12/14bit for RH/T) and a checksum helps to improve communication reliability.

With this set of features and the proven reliability and long-term stability, the SHT2x sensors offer an outstanding performance-to-price ratio. For testing SHT2x two evaluation kits EK-H4 and EK-H5 are available.

Dimensions

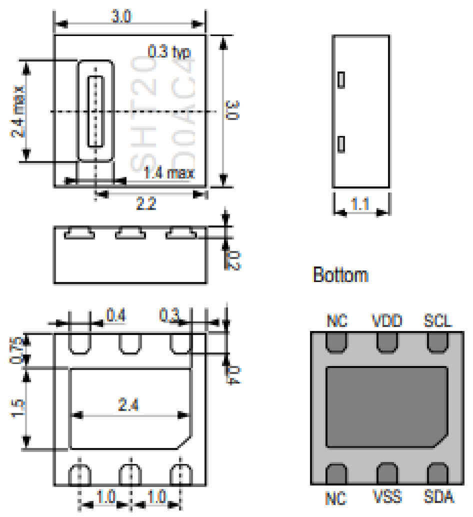

Figure 1: Drawing of SHT20 sensor package, dimensions are given in mm (1 mm = 0.039 inch), tolerances are ±0.1 mm. The die pad (center pad) is internally connected to VSS. The NC pads must be left floating. VSS = GND, SDA = DATA. Numbering of E/O pads starts at lower right corner (indicated by notch in die pad) and goes clockwise (compare Table 2).

Sensor Chip

SHT20 features a generation 4C CMOSens® chip. Besides the capacitive relative humidity sensor and the band gap temperature sensor, the chip contains an amplifier, A/D converter, OTP memory and a digital processing unit.

Material Contents

While the sensor itself is made of Silicon the sensors' housing consists of a plated Cu lead-frame and green epoxy-based mold compound. The device is fully RoHS and WEEE compliant, e.g. free of Pb, Cd and Hg.

Additional Information and Evaluation Kits

Additional informations such as Application Notes are available from the web page www.sensirion.com/products/catalog/SHT20. For more information please contact Sensirion via info@sensirion.com.

For SHT20 two Evaluation Kits are available: EK-H4, a four-channel device with Viewer Software, that also serves for data-logging, and a simple EK-H5 directly connecting one sensor via USB port to a computer.

SENSIRION
THE SENSOR COMPANY

Sensor Performance

Relative Humidity

Parameter	Condition	Value	Units
Resolution [1]	12 bit	0.04	%RH
	8 bit	0.7	%RH
Accuracy tolerance [2]	typ	±3.0	%RH
	max	see Figure 2	%RH
Repeatability		±0.1	%RH
Hysteresis		±1	%RH
Nonlinearity		<0.1	%RH
Response time [3]	τ 63%	8	s
Operating Range	extended [4]	0 to 100	%RH
Long Term Drift [5]	Typ.	< 0.25	%RH/yr

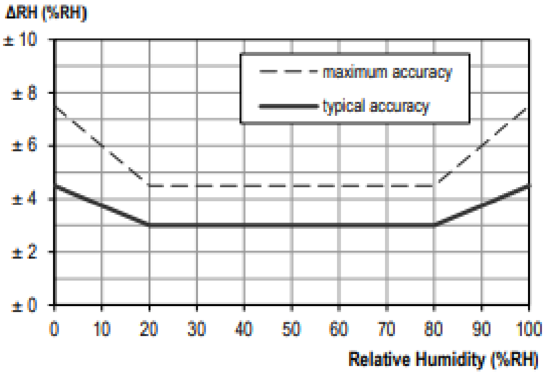

Figure 2 Typical and maximal tolerance at 25°C for relative humidity. For extensive information see Users Guide, Sect. 1.2.

Electrical Specification

Parameter	Condition	min	typ	max	Units
Supply Voltage, VDD		2.1	3.0	3.6	V
Supply Current, IDD [6]	sleep mode		0.15	0.4	μA
	measuring	200	300	330	μA
Power Dissipation [6]	sleep mode		0.5	1.2	μW
	measuring	0.6	0.9	1.0	mW
	average 8bit		3.2		μW
Heater	VDD = 3.0 V	5.5mW, ΔT = + 0.5-1.5°C			
Communication	digital 2-wire interface, I²C protocol				

Table 1 Electrical specification. For absolute maximum values see Section 4.1 of Users Guide.

Temperature

Parameter	Condition	Value	Units
Resolution [1]	14 bit	0.01	°C
	12 bit	0.04	°C
Accuracy tolerance [2]	typ	±0.3	°C
	max	see Figure 3	°C
Repeatability		±0.1	°C
Operating Range	extended [4]	-40 t0 125	°C
Response Time [7]	τ 63%	5 to 30	s
Long Term Drift[8]	Typ.	< 0.02	°C/yr

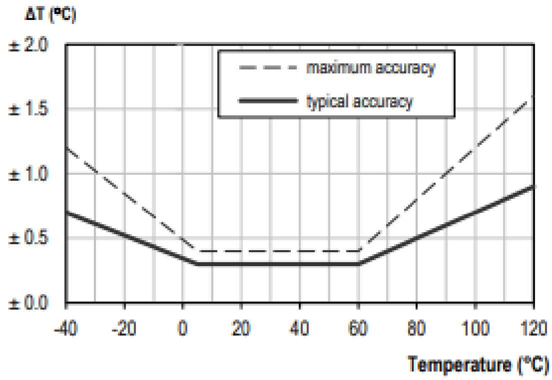

Figure 3 Typical and maximal tolerance for temperature sensor in °C.

Packaging Information

Sensor Type	Packaging	Quantity	Order Number
SHT20	Tape & Reel	1500	1-100706-01
	Tape & Reel	5000	1-100704-01

Please Note: This datasheet is subject to change and may be amended without prior notice.

[1] Default measurement resolution is 14bit (temperature) / 12bit (humidity). It can be reduced to 12/8bit, 11/11bit or 13/10bit by command to user register.
[2] Accuracies are tested at Outgoing Quality Control at 25°C and 3.0 V. Values exclude hysteresis and long term drift and are applicable to non-condensing environments only.
[3] Time for achieving 63% of a step function, valid at 25°C and 1 m/s airflow.
[4] Normal operating range: 0-80 %RH, beyond this limit sensor may read a reversible offset with slow kinetics (+3 %RH after 60 h at humidity >80 %RH). For more details please see Section 1.1 of the Users Guide.
[5] Typical value for operation in normal RH/T operating range. Max. value is < 0.5 %RH/y. Value may be higher in environments with vaporized solvents, out-gassing tapes, adhesives, packaging materials, etc. For more details please refer to Handling Instructions.
[6] Min and max values of Supply Current and Power Dissipation are based on fixed VDD = 3.0 V and T<60°C. The average value is based on one 8bit measurement per second.
[7] Response time depends on heat conductivity of sensor substrate.
[8] Max. value is < 0.04°C/y.

Users Guide SHT20

1 Extended Specification

For details on how Sensirion is specifying and testing accuracy performance please consult Application Note "Statement on Sensor Specification".

1.1 Operating Range

The sensor works stable within recommended Normal Range – see Figure 4. Long term exposure to conditions outside Normal Range, especially at humidity >80 %RH, may temporarily offset the RH signal (+3 %RH after 60 h). After return into the Normal Range it will slowly return towards calibration state by itself. Prolonged exposure to extreme conditions may accelerate ageing.

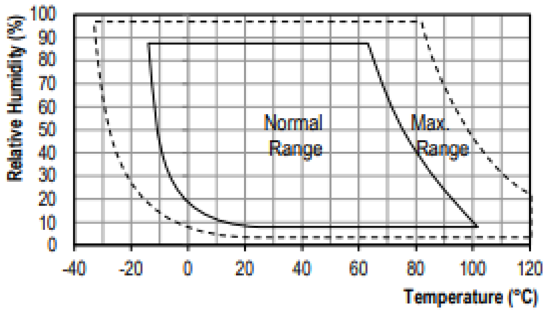

Figure 4 Operating Conditions

1.2 RH accuracy at various temperatures

Typical RH accuracy at 25°C is defined in Figure 2. For other temperatures, typical accuracy has been evaluated to be as displayed in Figure 5.

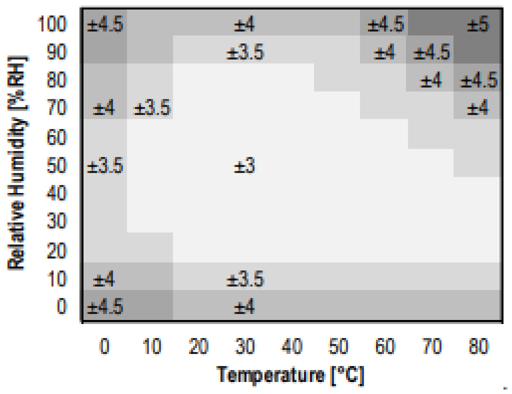

Figure 5 Typical accuracy of relative humidity measurements given in %RH for temperatures 0 – 80°C.

Please note that above values are maximal tolerances (not including hysteresis) against a high precision reference such as a dew point mirror. Typical deviations are at ±2 %RH where maximal tolerance is ±3% RH and about half the maximal tolerance at other values.

1.3 Electrical Specification

Current consumption as given in Table 1 is dependent on temperature and supply voltage VDD. For estimations on energy consumption of the sensor Figures 6 and 7 may be consulted. Please note that values given in these Figures are of typical nature and the variance is considerable.

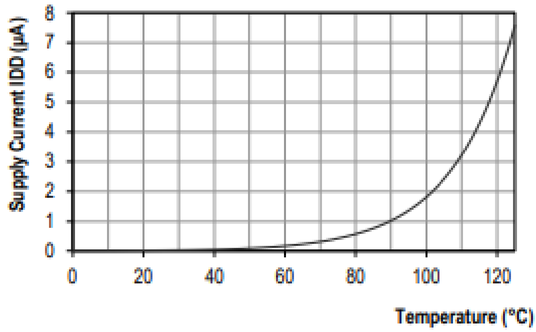

Figure 6 Typical dependency of supply current (sleep mode) versus temperature at VDD = 3.0 V. Please note that the variance of these data can be above ±25% of displayed value.

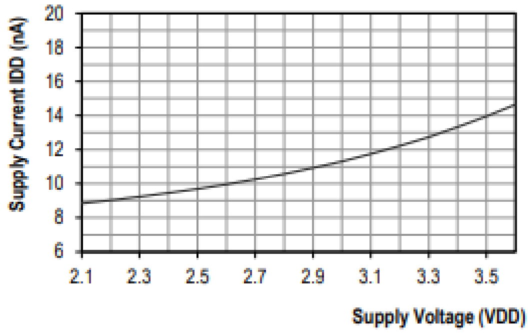

Figure 7 Typical dependency of supply current (sleep mode) versus supply voltage at 25°C. Please note that deviations may be up to ±50% of displayed value. Values at 60°C scale with a factor of about 15 (compare Table 1).

2 Application Information

2.1 Soldering Instructions

The *DFN's die pad* (centre pad) and *perimeter I/O pads* are fabricated from a planar copper lead-frame by over-molding leaving the die pad and I/O pads exposed for mechanical and electrical connection. Both the I/O pads and die pad should be soldered to the PCB. In order to prevent oxidation and optimize soldering, the bottom side of the sensor pads is plated with Ni/Pd/Au.

On the PCB the *I/O lands*[9] should be 0.2 mm longer than the package I/O pads. Inward corners may be rounded to match the I/O pad shape. The I/O land width should match the DFN-package I/O-pads width 1:1 and the land for the die pad should match 1:1 with the DFN package – see Figure 8.

The *solder mask*[10] *design* for the land pattern preferably is of type Non-Solder Mask Defined (NSMD) with solder mask openings larger than metal pads. For NSMD pads, the solder mask opening should be about 120 µm to 150 µm larger than the pad size, providing a 60 µm to 75 µm design clearance between the copper pad and solder mask. Rounded portions of package pads should have a matching rounded solder mask-opening shape to minimize the risk of solder bridging. For the actual pad dimensions, each pad on the PCB should have its own solder mask opening with a web of solder mask between adjacent pads.

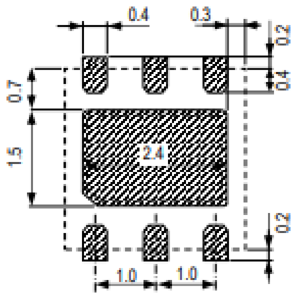

Figure 8 Recommended metal land pattern for SHT2x. Values in mm. Die pad (centre pad) may be left floating or be connected to ground, NC pads shall be left floating. The outer dotted line represents the outer dimension of the DFN package.

For *solder paste printing* a laser-cut, stainless steel stencil with electro-polished trapezoidal walls and with 0.125 mm stencil thickness is recommended. For the I/O pads the stencil apertures should be 0.1 mm longer than PCB pads and positioned with 0.1 mm offset away from the centre of the package. The die pad aperture should cover about 70 – 90% of the pad area – say up to 1.4 mm x 2.3 mm centered on the thermal land area. It can also be split in two openings.

Due to the low mounted height of the DFN, "no clean" type 3 solder paste[11] is recommended as well as Nitrogen purge during reflow.

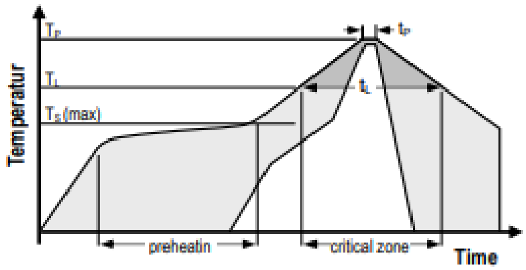

Figure 9 Soldering profile according to JEDEC standard. T_P <= 260°C and t_P < 30 sec for Pb-free assembly. T_L < 220°C and t_L < 150 sec. Ramp-up/down speeds shall be < 5°C/sec.

It is important to note that the diced edge or side faces of the I/O pads may oxidise over time, therefore a solder fillet may or may not form. Hence there is no guarantee for solder joint fillet heights of any kind.

For soldering SHT2x, standard *reflow soldering* ovens may be used. The sensor is qualified to withstand soldering profile according to IPC/JEDEC J-STD-020 with peak temperatures at 260°C during up to 30 sec for Pb-free assembly in IR/Convection reflow ovens (see Figure 9).

For manual soldering contact time must be limited to 5 seconds at up to 350°C.

Immediately after the exposure to high temperatures the sensor may temporarily read a negative humidity offset (typ. -1 to -2%RH after reflow soldering). This offset slowly disappears again by itself when the sensor is exposed to ambient conditions (typ. within 1-3 days). If RH testing is performed immediately after reflow soldering, this offset should be considered when defining the test limits.

In no case, neither after manual nor reflow soldering, a board wash shall be applied. Therefore, and as mentioned above, it is strongly recommended to use "no-clean" solder paste. In case of applications with exposure of the sensor to corrosive gases or condensed water (i.e. environments with high relative humidity) the soldering pads shall be sealed (e.g. conformal coating) to prevent loose contacts or short cuts.

[9] The land pattern is understood to be the metal layer on the PCB, onto which the DFN pads are soldered to.

[10] The solder mask is understood to be the insulating layer on top of the PCB covering the connecting lines.

[11] Solder types are related to the solder particle size in the paste: Type 3 covers the size range of 25 – 45 µm (powder type 42).